SEISMIC SOURCE LOCATIONS AND PARAMETERS FOR SPARSE NETWORKS BY MATCHING OBSERVED SEISMOGRAMS TO SEMI-EMPIRICAL SYNTHETIC SEISMOGRAMS

David H. Salzberg, Karen E. Votaw, and Margaret E. Marshall

SAIC Ocean Sciences Division

Sponsored by Air Force Research Laboratory

Contract No. FA8718-05-C-0019

ABSTRACT

The purpose of this study is to demonstrate the feasibility of full-waveform earthquake location using semi-empirical synthetic waveforms and received data from two or more regional stations.

Matching observed waveforms with synthetic waveforms has been used for some time in ocean acoustics to provide robust tracking of underwater sources in bearing, range and depth using synthetic pressure fields (e.g., Baggeroer et al., 1993). In such matched field processing, the pressure time series recorded by a dense array of hydrophones is steered using the synthetic pressure field predicted for a known environment. This approach is ideally suited for the ocean environment since the medium properties are well constrained. In contrast, the properties of the solid earth are not known at the detail required to perform matched field processing on seismic arrays for source location on a global scale. Matched waveform processing for seismic source locations has only been successfully applied when the overall velocity is well constrained (e.g., Pulliam et al., 2000).

Our method overcomes the uncertainty in the velocity models by generating semi-empirical synthetic seismograms. Empirical and semi-empirical approaches for modeling waveforms have been used to model waveforms from large events using smaller events as Green's functions (Wu, 1978). However, this approach breaks down when the two events are neither co-located nor have similar mechanisms. Others use semi-empirical synthetic seismograms, i.e., synthetic seismograms convolved with empirically determined source time functions, to estimate the ground motion of hypothetical events to assess earthquake hazards (e.g., Summerville et al., 2000). Salzberg (1996) developed a semi-empirical technique for fundamental mode surface waves which allows synthetic seismograms to be computed when the reference event is at a different location and has a different mechanism.

Our approach is to find the semi-empirical synthetic seismogram computed that best matches the observed seismic waveforms across a dense grid of possible locations. For each grid location, two or more waveforms are compared for a known moment tensor using the semi-empirical synthetic waveforms. The resulting minimum in the residual at the grid points yields the optimal location.

OBJECTIVE(S)

The objective of the research is to provide a method that gives accurate locations and source mechanisms using a sparse regional network when two or more seismic stations record the event. Tests using synthetic waveforms indicate that location accuracy on the order of 300-500 km^2 and depth uncertainty of less than 5 km can be obtained with recordings from only two stations low pass-filtered at 0.5 Hz. Since the fundamental constraint in matched waveform processing is the increasing incoherence between the complete waveforms with distance, sensor separation can be used to simulate event separation. Thus, examining full waveform correlations from a seismic array should provide a separate estimate of the ability to resolve the source location.

Methodology

SAIC is implementing a matched waveform approach to locate seismic events using a sparse regional network.

Matching observed waveforms with synthetic waveforms has been used for some time in ocean acoustics to provide robust estimates of underwater source locations in range, bearing and depth (Baggeroer et al., 1993) using synthetic pressure fields. In such matched field processing, the pressure time series recorded at each element of a tightly spaced an array of hydrophones correlated with the synthetic pressure field. The variation is the wave field resulting from interference patterns may be unique to the source location. By searching over a grid of potential sources, the optimal source location is identified by the maximum in correlation. This approach is ideally suited for the ocean environment since the medium properties are well constrained.

In contrast, the properties of the solid earth are not known at the detail required to perform matched field processing on seismic arrays for source location on a global scale. However, matching synthetic waveforms has been effectively applied in seismology to techniques such as inversion of the source and inversion of velocity models (Burdick and Langston, 1977). Waveform matching for source properties has been limited to regions with well constrained velocity models such as teleseismic body-waves which travel mostly in the lower mantle (Langston, 1981), long period surface waves (Romanowicz, 1981), and normal modes (Dziewonski et al., 1981). In these three examples, most of the energy propagates within the lower mantle. However, matched waveform processing for source locations, has only been successfully applied when the overall velocity is well constrained (Pulliam et al., 2000).

SAIC‘s method overcomes the uncertainty in the velocity models by generating semi-empirical synthetic seismograms. Empirical and semi-empirical approaches for modeling waveforms have been used to model waveforms from large events using smaller events as Green’s functions (Wu, 1978). This approach, however, breaks down if the two events are neither co-located nor have similar mechanisms. Others (e.g., Summerville et al., 2000) use semi-empirical synthetic seismograms, i.e., synthetic seismograms convolved with empirically determined source time functions, to estimate the ground motion of hypothetical events to assess earthquake hazards. Salzberg (1996) developed a semi-empirical technique for fundamental mode surface waves which allowed synthetic seismograms to be computed when the reference event is at a different source location and has a different mechanism. This technique provided coherent surface-waves at periods as short as 15 seconds, and allowed for the determination of moment tensor source mechanisms for small events (M > 4.7).

SAIC’s approach is to find the semi-empirical synthetic seismogram computed across a dense grid of possible locations that best matches the observed seismic waveforms. For each grid location, two or more 3-component waveforms are inverted for the moment tensor using the semi-empirical synthetic waveforms. The resulting minimum in the residual (χ^2 norm) from the moment tensor inversion results at the grid points yields the optimal location. .

Semi-Empirical Synthetics

When comparing the synthetic waveform with real data, a match is not possible unless the velocity model is well defined. Furthermore, errors in the synthetic waveforms translate into errors in the resolved location

and source parameters. Consequently, the primary limitation in matched waveform processing is the ability to produce high-fidelity simulations based on an idealized environmental model. One approach that can be used to improve the quality of the synthetic waveforms is to empirically determine the propagation portion of the synthetic waveform, yet still use the theoretical excitation (Salzberg, 1996; Velasco et al., 1994). These semi-empirical Green's Functions can be used to characterize the seismic wavefield recorded from sources in a reasonably homogeneous source region at a seismic station or array.

Semi-empirical Green's Functions are unnecessary if the source-to-receiver velocity structure is known perfectly, as full waveform synthetic seismograms are sufficient for matched waveform processing. However, only high-quality approximations of the velocity model can be determined. As such, any synthetic waveforms generated will only approximate the observed waveform written as:

$$observed\ (t) = u(t) * \Delta u(t) \tag{1}$$

where * represents the convolution operation, u is the synthetic waveform, and Δu is the mismatch of the data and synthetic represented as a filter. Δu corresponds to a systematic bias caused by model mismatch and an incoherent portion caused by random noise. The systematic portion of Δu can be written as:

$$\Delta u\ (\omega) = \Delta p(\omega) \cdot \Delta x(\omega) \tag{2}$$

where Δp is the mismatch caused by inaccuracies in the propagation, and Δx is the mismatch in the source excitation. The synthetic waveform, u, can be written as (Mendiguren, 1977):

$$u(r,\theta,h,\omega) = P(r,\omega) \cdot s(\omega) \cdot \sum_{i=1}^{5} H_i(\omega,\theta,h) \cdot m_i \tag{3}$$

where u is the far-field displacement, s is the source function, P is the propagation from source to receiver, H_i is the excitation function corresponding to m_i, and m_i is the i^{th} element of the moment tensor. Transferring Equation (1) into the frequency domain, and combining with Equations (2) and (3) can be combined to represent the observed seismogram as:

$$observed(\omega) = P(r,\omega) \cdot \Delta p(\omega) \cdot \left[s(\omega) \cdot \sum_{i=1}^{5} H_i(\omega,\theta,h) \cdot m \right] \cdot \Delta x(\omega) \tag{4}$$

In this formulation, the propagation term is mathematically separable from the source terms which include the moment tensor, excitation, and time functions. After deconvolving the source terms from the reference waveforms of known source mechanism, location, and depth, the source-to-receiver propagation is isolated as:

$$P(r,\omega) = \frac{reference(\omega)}{\left[s(\omega) \cdot \sum_{i=1}^{5} H_i(\omega,\theta,h) \cdot m_i \right] \cdot \Delta x(\omega) \cdot \Delta p(\omega)} \tag{5}$$

If a second event occurs close to the first event, then it reasonable to assume that the propagation from the second event to the receiver will be similar to the first event. The reference waveform can then be transferred to the mechanism and depth of the new waveform by substituting the empirical propagation determined in Equation (5) into observed waveform formulation in Equation (4). This result gives new waveform as

$$new(\omega) = \frac{reference(\omega)}{\left[\tilde{s}(\omega)\cdot\sum_{i=1}^{5}\tilde{H}_i(\omega,\theta,\tilde{h})\cdot\tilde{m}_i\right]\cdot\Delta\tilde{x}(\omega)\cdot\Delta\tilde{p}(\omega)}\cdot\left[\sum_{i=1}^{5}H_i(\omega,\theta,h)\cdot m_i\right]\cdot\Delta x(\omega)\cdot\Delta p(\omega) \tag{6}$$

where ~ over a variable indicates the reference waveform.

Accurate knowledge of the source moment tensor and excitation terms implies that the Δx terms are approximately 1. Furthermore, since the two events are in close proximity and assumed to have the same propagation, or $\Delta\tilde{p} = \Delta p$. Thus the new semi-empirical synthetic waveform is:

$$new(\omega) = \frac{reference(\omega)}{\left[\tilde{s}(\omega)\cdot\sum_{i=1}^{5}\tilde{H}_i(\omega,\theta,\tilde{h})\cdot\tilde{m}_i\right]}\cdot\left[\sum_{i=1}^{5}H_i(\omega,\theta,h)\cdot m_i\right] \tag{7a}$$

$$new(\omega) = \frac{reference(\omega)}{synthetic_{reference}(\omega)}\cdot synthetic_{new}(\omega) \tag{7b}$$

Conceptually, the formulation in (7b) assumes that the mismatch between the reference waveform and its synthetic waveform is identical to the mismatch between the new waveform and its corresponding synthetic waveform.

Examples

Two clusters from central and southern California were studied. This region was selected due to the quality of the catalog locations (GT2 or better), and the large number of regional stations. This particular study focuses on the Parkfield and Hector Mine events using data from two regional stations (TUC and ELK). In preliminary tests, semi-empirical Green's Functions and derived synthetics were computed on a 0.02^o x 0.02^o x 2 km grid, assuming that the reported focal mechanisms were correct. The results are listed Table 1.

Parkfield Event of Sept. 30, 2004 18:54:28

The reference event used for Parkfield was the 29-Sep-2004 17:10:04 aftershock. The match between the semi-empirical synthetic waveforms computed at each grid pint (.02 x .02 degree grid, 2 km in depth) and the observed waveforms indicates the optimal source location (upper left). As shown in Figure 1, this location is within 5 km of the ground-truth location, and a significant improvement over a location 11 km from ground truth reported by the CTBTO IDC. However, the event was also within 8 km of the location of the reference event. The optimal depth at each horizontal grid point, shown in Figure 2, was determined by finding the depth of the minimum residual at each point. However, this shows considerable variability , at the minimum residual shown in the upper right, where the optimal depth of 12 km is close to the ground truth depth of 10.43 km. In Figure 3, the observed waveform shows an excellent agreement to the semi-empirical synthetic waveform ().

Hector Mine Event of October 16, 1999 17:38

Matching the waveforms the Hector Mine aftershock relative to another Hector Mine Aftershock of October 22 at 16:08:48 yields an optimal source location which is within 8 km of the ground-truth location even though the event was 50 km from the reference event (Figure 4). In this case, the CTBTO PIDC system did not locate this event.

CONCLUSION(S) AND RECOMMENDATION(S)

In this preliminary study, we have demonstrated the ability to accurately locate events by matching semi-empirical synthetic waveforms to observed data using two regional broad-band stations. Assumptions implicit in the analysis are that the source mechanism for the event is known and there is a reference event available to generate the semi-empirical synthetic waveforms. In both cases listed in the table below, the two-station optimal location was within 8 km of ground-truth. Of particular importance is that our solution was closer to the ground truth location than the IDC REB solution.It should be noted that we accomplished these results using a global earth structure and published source mechanisms. After incorporating more appropriate regional velocity models and refined source inversions, the accuracy and robustness of the technique should improve significantly.

RESEARCH ACCOMPLISHED

- Refined Methodology; tested in 3-D for Parkfield and Hector Mine Aftershocks
- Collected Data for 218 Events in Southern and Central California (Figure 5)
- Reviewed the available data to identify those with usable signals

Work in the next 12 months:

- Measure the Group Velocity Curves or all reviewed waveforms
- Cluster the event to common group velocity curves at each station
- Define a set of master/reference events for each cluster
- Determine the 1-d path specific velocity models
- Generate Semi-Empirical Synthetics for the grid spacing
- Execute to grid search

ACKNOWLEDGEMENTS(S)

All waveform data was obtained from the IRIS DMC. The IDC event locations were from the SMDC Monitoring Research Web Page.

REFERENCE(S)

Aki, K. and P. G. Richard, (1980), *Quantitative Seismology: Theory and Methods, Volume 1*, W. H. Freeman and Company.

Baggeroer, A. B., W. A. Kuperman, and Peter N. Mikhalesky (1993), An Overview of Matched Field Methods in Ocean Acoustics, *IEEE Journal of Ocean Engineering*, 18: 401–424.

Dziewonski, A. M., A. T. Chou, and J. H. Woodhouse (1981). Determination of Earthquake Source Parameters from Waveform Data for Studies of Global and Regional Seismicity, *J. Geophys. Res.* 86: 2825–2852.

Herrmann, R. H. and C. A. Ammon, (2002) Computer Programs in Seismology: Surface Waves, Receiver Functions and Crustal Structure.

Kanamori, H., and J. W. Given (1982), Use of Long-Period Surface Waves for Rapid Determination of Earthquake Source Parameters 2. Preliminary Determination of Source Mechanisms of Large Earthquakes (M_S > 6.5) in 1980, *Phys. Earth and Planetary Int.* 30: 260-268.

Kennett, B., and Engdahl, E. (1991), Traveltimes for global earthquake location and phase identification, *Geophys. J. Int.* 105: 429–465.

Langston, C. A. (1981), Source Inversion of Seismic Waveforms: The Konya, India Earthquake of September 13, 1967, *Bull. Seism. Soc. Am* 71**:** 1–24.

Langston, C.A., and D. V. Helmberger (1975), A Procedure for Modeling Shallow Dislocation Sources, *Geophys. Journ. R. A. S*. 42: 117–130.

Lay, T. and T. C. Wallac (1995), *Modern Global Seismology*, Academic Press, San Diego, California.

Mendiguren, J. A. (1977), Inversion of Surface Wave Data in Source Mechanism Studies, *J. Geophs. Res.* 78: 889–894.

Patton, H. J. and G, Zandt (1980), Seismic Moment Tensors of Western U. S. Earthquakes and Implications fir the Tectonic Stress Field, *J. Geophys. Res.* 85: 821–848.

Press, W. H., B. P. Flannery, S. A., Teukolsky, and W.T. Vetterling (1986), *Numerical Recipes: The Art of Scientific Computing*, Cambridge University Press, Cambridge, England.

Pulliam, J. , C. Frohlich, and B. Phillips (2000), Single Station Event Location:
Epicentral Distance, Bearing, and Focal Depth, DOE Seismic Research Symposium.

Salzberg, David. H. (1996), *Simultaneous inversion of moderate earthquakes using body and surface waves: methodology and applications to the study of the tectonics of Taiwan*, Ph.D. Thesis, The State University of New York at Binghamton, Binghamton, NY.

Savage, B. J. Chen, and D. V. Helmberger (2003), Seismic Velocity Variations beneath the Southern Sierra Nevada and the Walker Lane, *J. Geophs. Res.* 108: 2325–2341.

Summerville, P. R. Graves and N. Collins (2000), Ground Motions for Site Response Estimates – 1906 Earthquake, Technical Report to the Pacific Earthquake Engineering Research Center.

Velasco, A.A., C.J. Ammon, and T. Lay (1994), Recent Large Earthquakes Near Cape Mendocino and in the Gorda Plate: Broadband Source Time Functions, Fault Orientations and Rupture Complexities, *J. Geophys. Research* 99: 711–728.

Wu, F. T. (1978), Prediction of String Ground Motion Using Small Earthquakes, *Proceedings of the 2nd International Conference on Microzonation,* National Science Foundation, San Francisco, CA, 701–704.

Table 1. The relocated event locations compared with catalog events.

Time	Name	GT Lat	GT Lon	GT Depth	WF Lat	WF Lon	WF Depth	Error	IDC Lat	IDC Lon
2004/09/30 18:54	Parkfield	35.9885	-120.5387	10.43	35.96	-120.54	12	3.2	36.0283	-120.4298
1999/10/16 17:38	Hector Mine	34.43	-116.252	N/A	34.36	-116.26	14	7.8	N/A	N/A

Figure 1. Map Minimum Residual for the Parkfield test Case

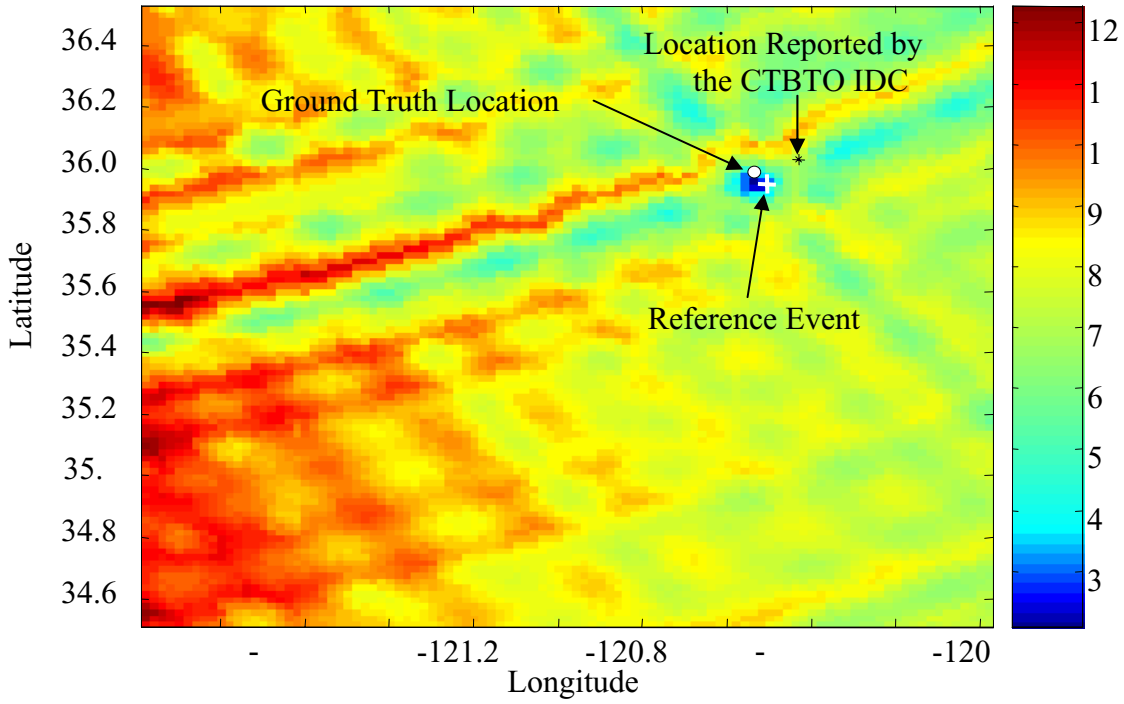

Figure 2. Residual vs. Depth for the Parkfield test Case

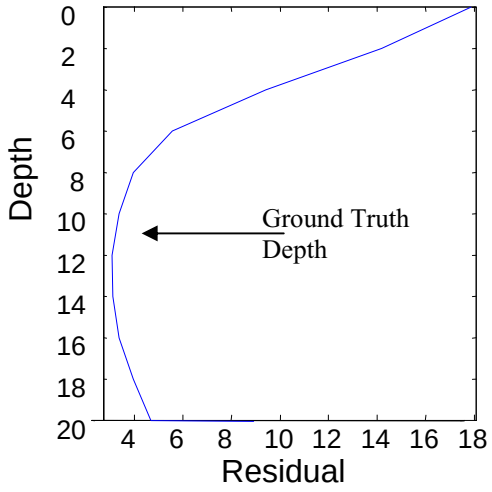

Figure 3. Comparison of Data and Synthetic for Parkfield Test Case

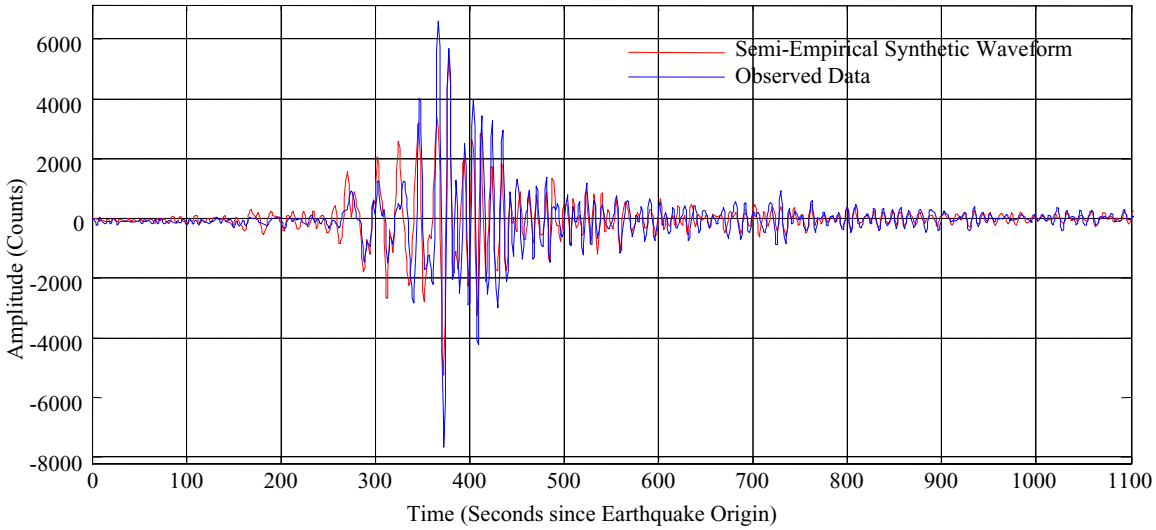

Figure 4. Map Minimum Residual for the Hector Mine test case

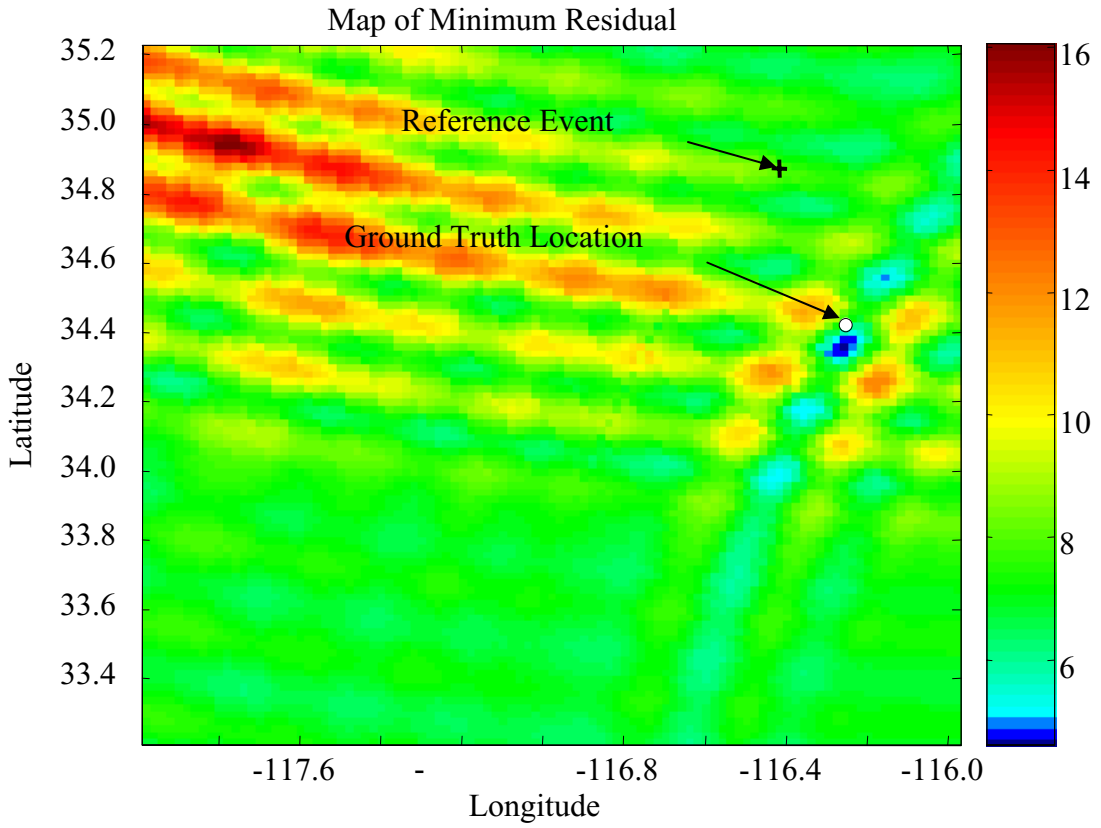

Figure 5. Event groupings in the study